

Enantioselective Hydrogenation Catalysis Aided by a σ -Bonded Calix[4]arene to a *P*-Chirogenic Aminophosphane Phosphinite Rhodium Complex[†]

Naïma Khiri,[‡] Etienne Bertrand,^{‡,§} Marie-Joëlle Ondel-Eymin,[‡] Yoann Rousselin,[‡]
Jérôme Bayardon,[‡] Pierre D. Harvey,^{*,§} and Sylvain Juge^{*,‡}

[‡]*Institut de Chimie Moléculaire de l'Université de Bourgogne, UMR CNRS 5260, 9 Avenue Alain Savary BP 47870, 21078 Dijon Cedex, France, and* [§]*Département de Chimie, Université de Sherbrooke, Sherbrooke, Québec, Canada J1K 2R1*

Received May 27, 2010

The first *P*-chirogenic aminophosphane–phosphinite (AMP*P) ligand (**4a**) supported on the upper rim of a calix[4]arene moiety was synthesized in two steps using the ephedrine methodology. Ligand **4a** was used for the preparation of the corresponding rhodium complex [Rh(COD)-(AMP*P)]BF₄ (**5a**) (COD = 1,8-cyclooctadienyl), which was tested for asymmetric catalyzed hydrogenation of various substrates. The structures of the AMP*P ligand as diborane and rhodium complexes **3a** and **5a** were established by X-ray analysis. The asymmetric hydrogenation catalyzed with the Rh complex **5a** exhibits excellent enantioselectivities up to 98%. Investigation of modified *P*-chirogenic aminophosphane–phosphinite ligands **4b,c**, bearing an isoelectronic or a sterically similar substituent on the *P*-chirogenic aminophosphane unit, demonstrates that the calix[4]arene substituent of the aminophosphane moiety plays a major role in the better asymmetric induction. The enantioselectivity of the catalyzed hydrogenation was weakly influenced by the hydrogen pressure, which is in good agreement with a stereodetermining step involving the substrate–rhodium complexes. Computer modeling indicated the presence of two conformers for the active AMP*P rhodium species, according to whether the rhodium metal is outside or inside the calix[4]arene cavity (called *outer* and *inner*). It is obvious that the complexation of the substrate with the active rhodium species forces this complex to adopt fully the *outer* conformation and hence explains why the calixarene fragment plays a key role in the stereodetermining step.

Introduction

Asymmetric catalysis using chiral transition metal complexes is a powerful method for the synthesis of chiral substances, in laboratory scale as well as industrially.^{1–4} So far, mostly chiral catalysts were prepared by complexation of a chiral organophosphorus ligand and a transition metal.^{5,6} However, improving an asymmetric catalytic reaction for a new substrate is never trivial and is mainly

restricted by the availability of a library of chiral ligands⁷ or by the structure modification of an efficient lead series such as BINAP,⁸ DUPHOS,⁹ PHOX,¹⁰ monophos,¹¹ bisP*,¹² and SDP.¹³

Aminophosphane phosphinites (AMPP) are also convenient chiral ligands capable of improving highly stereoselective

[†] This paper is dedicated to Prof. H. Kagan for his 80th birthday.

*To whom correspondence should be addressed. E-mail: Sylvain.Juge@u-bourgogne.fr. Tel: +33 (0)3 80 39 61 13. E-mail: Pierre.Harvey@USherbrooke. Tel: 1-819-821-7092.

(1) Ojima, I. *Catalytic Asymmetric Synthesis*, 2nd ed.; Wiley-VCH: Weinheim, 2000.

(2) Jacobsen, E. N.; Pfaltz, A.; Yamamoto, H. *Comprehensive Asymmetric Catalysis*; Springer: New York, 2000.

(3) (a) Blaser, H. U.; Spindler, F.; Studler, M. *Appl. Catal. A: Gen.* **2001**, 221, 119–143. (b) Blaser, H. U.; Malan, C.; Pugin, B.; Spindler, F.; Steiner, H.; Studer, M. *Adv. Synth. Catal.* **2003**, 345, 103–151. (c) Blaser, H. U.; Schmidt, E. *Asymmetric Catalysis on Industrial Scale*; Wiley-VCH: Weinheim, 2003. (d) Blaser, H. U.; Pugin, B.; Spindler, F.; Tommen, M. *Acc. Chem. Res.* **2007**, 40, 1240–1250.

(4) Johnson, N. B.; Lennon, I. C.; Moran, P. H.; Ramsden, J. A. *Acc. Chem. Res.* **2007**, 40, 1291–1299.

(5) Tang, W.; Zang, X. *Chem. Rev.* **2003**, 103, 3029–3069.

(6) Jäkel, C.; Paciello, R. *Chem. Rev.* **2006**, 106, 2912–2942.

(7) Zhang, W.; Chi, Y.; Zhang, X. *Acc. Chem. Res.* **2007**, 40, 1278–1290.

(8) Berthod, M.; Mignani, G.; Woodward, G.; Lemaire, M. *Chem. Rev.* **2005**, 105, 1801–1836.

(9) Clark, T. P.; Landis, C. R. *Tetrahedron: Asymmetry* **2004**, 15, 2123–2137.

(10) Hargaden, G. C.; Guiry, P. J. *Chem. Rev.* **2009**, 109, 2505–2550.

(11) (a) van den Berg, M.; Minnaard, A. J.; Schudde, E. P.; van Esch, J.; de Vries, A. H. M.; de Vries, J. G.; Feringa, B. L. *J. Am. Chem. Soc.* **2000**, 122, 11539–11540. (b) van den Berg, M.; Minnaard, A. J.; Haak, R. M.; Leeman, M.; Schudde, E. P.; Meetsma, A.; Feringa, B. L.; de Vries, A. H. M.; Maljaars, C. E. P.; Hyett, D.; Willans, C. E.; Boogers, J. A. F.; Henderickx, H. J. W.; de Vries, J. G. *Adv. Synth. Catal.* **2003**, 345, 308–323.

(12) (a) Crépy, K. V. L.; Imamoto, T. *Top. Curr. Chem.* **2003**, 229, 1–40. (b) Imamoto, T. *J. Synth. Org. Chem., Jpn.* **2007**, 65, 1060–1069.

(13) Xie, J.-H.; Zhou, Q.-L. *Acc. Chem. Res.* **2008**, 41, 581–593.

(14) (a) Kreuzfeld, H. J.; Schmidt, U.; Döbler, C.; Krause, H. W. *Tetrahedron: Asymmetry* **1996**, 7, 1011–1018. (b) Agbossou, F.; Carpentier, J. F.; Hapiot, F.; Suisse, I.; Mortreux, A. *Coord. Chem. Rev.* **1998**, 178–180, 1615–1645. (c) Broger, E. A.; Burkart, W.; Hennig, M.; Scalone, M.; Schmidt, R. *Tetrahedron: Asymmetry* **1998**, 9, 4043–4054. (d) Lot, O.; Suisse, I.; Mortreux, A.; Agbossou, F. *J. Mol. Catal. A* **2000**, 164, 125–130. (e) Chen, G.; Li, X.; Gang, L.; Mi, A.; Cui, X.; Jiang, Y.; Choi, M. C. K.; Chan, A. S. C. *Tetrahedron: Asymmetry* **2002**, 13, 809–813. (f) Dubrovina, N. V.; Tararov, V. I.; Kadyrova, Z.; Monsees, A.; Börner, A. *Synthesis* **2004**, 12, 2047–2051.

catalysis, because libraries of such compounds can easily be synthesized from available chiral amino alcohols in a few steps.^{14–16} Numerous works have demonstrated the efficiency of the synthesis of chiral AMP*P ligands that can be applied to asymmetric catalyses from their corresponding Rh, Ru, Pd, or Ni complexes.^{14b,16,17} Recently, we and other groups have independently described a series of *P*-chirogenic AMP*P ligands derived from ephedrine, for catalytic asymmetric hydrogenation and hydroformylation reactions involving rhodium complexes^{18,19}

Over the past decades, phosphorus ligands containing calix[*n*]arenes have also received extensive attention for their coordination chemistry and in transition metal catalysis.²⁰ The use of calix[4]arene-based phosphorus ligands in catalysis has been more recently recognized for their potential

applications and has already been evaluated in olefin hydroformylation,²¹ oligomerization and polymerization reactions,²² hydrogenation,^{21a,23} olefin oxidation,²⁴ carbon–carbon bond forming reactions,²⁵ and allylic alkylation.²⁶

So far, many chiral organophosphorus ligands derived from calix[*n*]arene are known,^{20–26} but only a few asymmetric catalyses were described.²³ We now report herein the first stereoselective synthesis of a *P*-chirogenic AMP*P ligand with a calix[4]arene as substituent of the aminophosphane moiety along with an investigation of a Rh(I)-catalyzed asymmetric hydrogenation. It is clearly demonstrated that the calix[4]arene plays a key role in the enantioselectivity.

Results and Discussion

P-Chirogenic aminophosphane–phosphinite ligand **4a** is prepared in two steps from the (+)-oxazaphospholidine borane **1**, derived from (–)-ephedrine, according to the general procedure described for the AMP*P.¹⁹ The reaction of the starting complex **1** with the 25,26,27,28-tetrapropoxycalix[4]aren-5-yl lithium reagent leads, after P–O bond cleavage, to the ring-opening alcoholate intermediate **2a**, which is trapped with chlorodiphenylphosphane. Subsequently, it is further trapped with borane to afford the AMP*P in 62% yield as diborane complex **3a** (Scheme 1).

The structure of the calix[4]arene-containing AMP*P diborane **3a** has been determined by X-ray diffraction methods, and the ORTEP view is shown in Figure 1. The calix[4]arene substituent adopts a flattened cone conformation in the solid state due to the presence of the propoxy groups in the lower rim. The compound exhibits an unfolded conformation of the AMP*P chain with a flattened nitrogen pyramidal structure and the P–B bonds disposed *anti* from one another. The unit cell contains four independent molecules with similar conformations. The *S* absolute configuration of the aminophosphane borane fragment is consistent with the retention of configuration previously reported for

(15) (a) Petit, M.; Morteux, A.; Petit, F.; Buono, G.; Pfeiffer, G. *New J. Chem.* **1983**, 7, 583–586. (b) Brunner, H.; Zettlmeir, W. *Handbook of Enantioselective Catalysis with Transition Metal Compounds, Ligands*, Vol. 2; VCH: Weinheim, 1993.

(16) Agbossou-Niedercorn, F.; Suisse, I. *Coord. Chem. Rev.* **2003**, 242, 145–158.

(17) Goudriaan, P. E.; van Leeuwen, P. W. N. M.; Birkholz, M.-N.; Reek, J. N. H. *Eur. J. Inorg. Chem.* **2008**, 2939–2958.

(18) (a) Ewalds, R.; Eggeling, E. B.; Alison, C. H.; Kamer, P. C.; van Leeuwen, P. W. N. M.; Vogt, D. *Chem.—Eur. J.* **2000**, 6, 1496–1506. (b) Carbó, J. J.; Liedós, A.; Vogt, D.; Bo, C. *Chem.—Eur. J.* **2006**, 12, 1457–1467. (c) den Heeten, R.; Swennenhuis, B. H. G.; van Leewen, P. W. N. M.; de Vries, J. G. *Angew. Chem., Int. Ed.* **2008**, 47, 1–5.

(19) (a) Moulin, D.; Darcel, C.; Jugé, S. *Tetrahedron: Asymmetry* **1999**, 10, 4729–4743. (b) Darcel, C.; Moulin, D.; Henry, J.-C.; Lagrelette, M.; Richard, P.; Harvey, P. D.; Jugé, S. *Eur. J. Org. Chem.* **2007**, 2078–2090.

(20) (a) Wieser, C.; Dieleman, C. B.; Matt, D. *Coord. Chem. Rev.* **1997**, 165, 93–161. (b) Dieleman, D.; Marsol, C.; Matt, D.; Kyritsakas, N.; Harriman, A.; Kintzinger, J.-P. *J. Chem. Soc., Dalton Trans.* **1999**, 4139–4148. (c) Lejeune, M.; Jeunesse, C.; Matt, D.; Kyritsakas, N.; Welter, R.; Kintzinger, J.-P. *J. Chem. Soc., Dalton Trans.* **2002**, 1642–1650. (d) Gutsche, C. D. *Calixarenes: An Introduction, Monographs in Supramolecular Chemistry*; Royal Society of Chemistry: Cambridge, 2008. (e) Homden, D. M.; Redshaw, C. *Chem. Rev.* **2008**, 108, 5089–5130. (f) Silwa, W.; Kozłowski, C. *Calixarenes and Resorcinarenes: Synthesis, Properties and Applications*; Wiley-VCH, 2009.

(21) (a) Wieser, C.; Matt, D.; Fischer, J.; Harriman, A. *J. Chem. Soc., Dalton Trans.* **1997**, 2391–2402. (b) Csók, Z.; Szalontai, G.; Czira, G.; Kollár, L. *J. Organomet. Chem.* **1998**, 570, 23–29. (c) Paciello, R.; Siggel, L.; Röper, M. *Angew. Chem. Ed.* **1999**, 38, 1920–1923. (d) Cobley, C. J.; Ellis, D. D.; Orpen, A. G.; Pringle, P. G. *J. Chem. Soc., Dalton Trans.* **2000**, 1109–1112. (e) Parlevliet, F. J.; Kiener, C.; Fraanje, J.; Goubitz, K.; Lutz, M.; Spek, A. L.; Kamer, P. C. J.; van Leeuwen, P. W. N. M. *J. Chem. Soc., Dalton Trans.* **2000**, 1113–1122. (f) Shirakawa, S.; Shimizu, S.; Sasaki, Y. *New J. Chem.* **2001**, 25, 777–779. (g) Kunze, C.; Selent, D.; Neda, I.; Schmutzler, R.; Spannenberg, A.; Börner, A. *Heteroat. Chem.* **2001**, 12, 577–585. (h) Steyer, S.; Jeunesse, C.; Matt, D.; Welter, R.; Wesolek, M. *J. Chem. Soc., Dalton Trans.* **2002**, 4264–4274. (i) Plourd, F.; Gilbert, K.; Gagnon, J.; Harvey, P. D. *Organometallics* **2003**, 22, 2862–2875. (j) Steyer, S.; Jeunesse, C.; Harrowfield, J.; Matt, D. *J. Chem. Soc., Dalton Trans.* **2005**, 1301–1309. (k) Sémeril, D.; Matt, D.; Toupet, L. *Chem.—Eur. J.* **2008**, 14, 7144–7155. (l) Monnerau, L.; Sémeril, D.; Matt, D.; Toupet, L. *Adv. Synth. Catal.* **2009**, 351, 1629–1636.

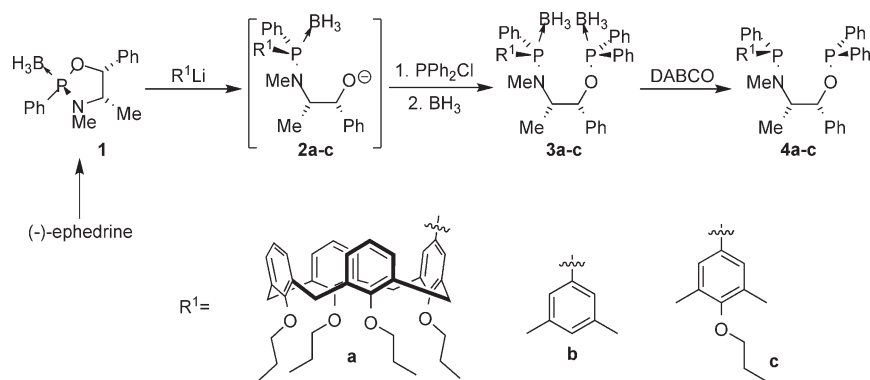
(22) (a) Parlevliet, F. J.; Zuideveld, M. A.; Kiener, C.; Kooijman, H.; Spek, A. L.; Kamer, P. C. J.; van Leeuwen, P. W. N. M. *Organometallics* **1999**, 18, 3394–3405. (b) Kemp, A.; Brown, D. S.; Lattman, M.; Li, J. J. *Mol. Catal. A* **1999**, 149, 125–133. (c) Zheng, Y. S.; Shen, Z. Q. *Eur. Polym. J.* **1999**, 35, 1037–1042. (d) Zheng, Y. S.; Ying, L. Q.; Shen, Z. Q. *Polymer* **2000**, 41, 1641–1643. (e) Gibson, V. C.; Redshaw, C.; Elsegood, M. R. *J. Chem. Soc., Dalton Trans.* **2001**, 767–769. (f) Chen, Y.; Zhang, Y.; Shen, Z.; Kou, R.; Chen, L. *Eur. Polym. J.* **2001**, 37, 1181–1184. (g) Capacchione, C.; Neri, P.; Proto, A. *Inorg. Chem. Commun.* **2003**, 6, 339–342. (h) Lejeune, M.; Sémeril, D.; Jeunesse, C.; Matt, D.; Peruch, F.; Lutz, P. J.; Ricard, L. *Chem.—Eur. J.* **2004**, 10, 5354–5360. (i) Huang, C.; Ahn, J.; Kwon, S.; Kim, J.; Lee, J.; Han, Y.; Kim, H. *Appl. Catal. A: Gen.* **2004**, 258, 173–181. (j) Kuhn, P.; Jeunesse, C.; Sémeril, D.; Matt, D.; Lutz, P.; Welter, R. *Eur. J. Inorg. Chem.* **2004**, 4602–4607. (k) Lejeune, M.; Sémeril, D.; Jeunesse, C.; Matt, D.; Lutz, P.; Toupet, L. *Angew. Chem., Int. Ed.* **2006**, 45, 881–886. (l) Redshaw, C.; Rowan, M. A.; Warford, L.; Homden, D. M.; Arbaoui, A.; Elsegood, M. R. J.; Dale, S. H.; Yamato, T.; Casas, C. P.; Matsui, S.; Matsuura, S. *Chem.—Eur. J.* **2007**, 13, 1090–1107.

(23) (a) Dieleman, C.; Steyer, S.; Jeunesse, C.; Matt, D.; Lutz, P.; Welter, R. *J. Chem. Soc., Dalton Trans.* **2001**, 2508–2517. (b) Marson, A.; Freixa, Z.; Kamer, P. C. J.; van Leeuwen, P. W. N. M. *Eur. J. Inorg. Chem.* **2007**, 4587–4591.

(24) (a) Li, Z.; Jablonski, C. *Chem. Commun.* **1999**, 1531–1532. (b) Massa, A.; D'Ambrosi, A.; Proto, A.; Scettri, A. *Tetrahedron Lett.* **2001**, 42, 1995–1998. (c) Karakhanov, E.; Buchneva, T.; Maximov, A.; Zavertyayeva, M. *J. Mol. Catal. A* **2002**, 184, 11–17. (d) Karakhanov, E.; Maksimov, A. L.; Runova, E. A.; Kardasheva, Y. S.; Terenina, M. V.; Buchneva, T. S.; Guchkova, Ya. A. *Macromol. Symp.* **2003**, 204, 159–173. (e) Maksimov, A. L.; Buchneva, T. S.; Karakhanov, E. A. *J. Mol. Catal. A* **2004**, 217, 59–67.

(25) (a) Ozerov, O. V.; Ladipo, F. T.; Patrick, B. O. *J. Am. Chem. Soc.* **1999**, 122, 7941–7942. (b) Ozerov, O. V.; Patrick, B. O.; Ladipo, F. T. *J. Am. Chem. Soc.* **2000**, 122, 6423–6431. (c) Morohashi, N.; Hattori, T.; Yokomakura, K.; Kabuto, C.; Miyano, S. *Tetrahedron Lett.* **2002**, 43, 7769–7772. (d) Seitz, J.; Mass, G. *Chem. Commun.* **2002**, 338–339. (e) Ladipo, F. T.; Sarveswaran, V.; Kingston, J. V.; Huyck, R. A.; Bylikin, S. Y.; Carr, S. D.; Watts, R.; Parkin, S. *J. Organomet. Chem.* **2004**, 689, 502–514. (f) Frank, M.; Mass, G.; Schatz, J. *Eur. J. Org. Chem.* **2004**, 607–613. (g) Sémeril, D.; Lejeune, M.; Jeunesse, C.; Matt, D. *J. Mol. Catal. A* **2005**, 239, 257–262. (h) Monnerau, L.; Sémeril, D.; Matt, D.; Toupet, L. *Adv. Synth. Catal.* **2009**, 351, 1383–1389. (i) Shirakawa, S.; Kimura, T.; Murata, S.; Shimizu, S. *J. Org. Chem.* **2009**, 74, 1288–1296.

(26) (a) Jeunesse, C.; Dieleman, C.; Steyer, S.; Matt, D. *J. Chem. Soc., Dalton Trans.* **2001**, 881–892. (b) Gibson, C.; Rebek, J., Jr. *Org. Lett.* **2002**, 4, 1887–1890. (c) Gaeta, G.; De Rosa, M.; Fruiro, M.; Soriente, A.; Neri, P. *Tetrahedron: Asymmetry* **2005**, 16, 2333–2340. (d) Sémeril, D.; Jeunesse, C.; Matt, D.; Toupet, L. *Angew. Chem., Int. Ed.* **2006**, 45, 5810–5814. (e) Sarkar, A.; Nethaji, M.; Krishnamurthy, S. S. *J. Organomet. Chem.* **2008**, 693, 2097–2110.

Scheme 1. Synthesis of the *P*-Chirogenic Aminophosphane–Phosphinite Ligands **4a–c**

the ring-opening cleavage of the starting complex **1** on treatment with an organolithium reagent (Scheme 1).¹⁹

The decomplexation of borane complex **3a** was achieved with retention of configuration on the phosphorus atom, upon heating with 1,4-diazabicyclo[2.2.2]octane (DABCO) in toluene at 50 °C. The free uncoordinated *P*-chirogenic aminophosphane–phosphinites **4a** was then obtained by short filtration on neutral alumina (Scheme 1).

In order to investigate the role of the calix[4]arene backbone in asymmetric induction, two AMP*P ligand models, **4b** and **4c**, bearing isoelectronic or sterically similar substituents, were prepared using the same methodology starting from (–)-ephedrine described above (Scheme 1). Thus, the AMP*P **4b** and **4c** were obtained with overall yields of 42% and 25%, respectively, by reaction of the corresponding *m*-xylyl- or *m*-dimethyl-*p*-propoxyphenyllithium reagent R¹Li with the (+)-oxazaphospholidine borane complex **1** (Scheme 1).

The three *P*-chirogenic aminophosphane–phosphinites **4a–c** were then tested as ligands in the rhodium-catalyzed asymmetric hydrogenation of various prochiral substrates **6** (Tables 1, 2). The [Rh(COD)₂]BF₄ precursor was used to prepare the corresponding chiral Rh complexes with the AMP*P ligands **4a–c**. The reaction of 0.9 equiv of [Rh(COD)₂]BF₄ with the ligands **4a–c** in dichloromethane provides the cationic rhodium complexes [Rh(COD)(AMP*P)]-BF₄ **5a–c** as air-stable orange powders, in good to excellent yields (52–92%; Scheme 2). The structure of the cationic complex **5a** was established by X-ray crystallography, and the ORTEP view is shown in Figure 2. The *P*-chirogenic aminophosphane moiety shows the *R* absolute configuration, which proves the retention of configuration of the decomplexation for AMP*P-diborane **4a**. On the other hand, the coordination sphere about the rhodium atom exhibits a distorted square-planar geometry with a P1–Rh–P2 angle of 91.18(5)°, and two other vertices are coordinated by the 1,5-cyclooctadiene η²-bonded double bonds. The dihedral angles between the planes defined by P1–Rh–P2 and either C72–Rh–C76 or C71–Rh–C75 are 8.15(21)° and 42.10(15)°, respectively. Interestingly, the seven-membered Rh–AMP*P chelate ring adopts a boat-like conformation, with a slight distortion of –12.71(38)° for the O1–C13–N1–P2 dihedral angle and where the substituents of the ephedrine backbone (*i.e.*, Ph, Me) are located at the equatorial positions. As a consequence, the H–C20 bond points in the direction of the rhodium atom with a H···Rh distance of 2.913 Å. Noteworthy, the sum of the angles around the N atom (*i.e.*, 356.57°) indicates an almost flattened geometry, which places the C22 methyl group on a side face of the tetrahedral phosphorus center and in the *anti* position with respect to the

P2–Rh bond. This conformation features the C7 and C23 phenyl phosphorus substituents in axial positions, but the distortion of the chelated ring induces a clear facial dissymmetry for the complex. In addition, the presence of the C22 methyl group and cyclooctadiene ligand forces the calix[4]arene group to be situated in the *syn* position in relation to the P2–C23 axial bond.

First, the rhodium-catalyzed asymmetric hydrogenation of methyl 2-acetamidocinnamate **6a** was used to determine the catalytic behavior of the new *P*-chirogenic AMP*P ligand **4a**. Initial hydrogenation experiments were performed at 1 bar of hydrogen pressure in methanol, using 3 mol % of [Rh(COD)(AMP*P)]BF₄ **5a**. In these conditions, the hydrogenation of the substrate **6a** was total, and the (*R*)-*N*-acetylphenylalanine methyl ester **7a** was obtained with 76% ee (Table 1, entry 1). This relative high ee compelled us toward further optimization. The influence of the solvent on the enantioselectivity was then investigated, as previously reported by many authors,²⁷ and the results are also summarized in Table 1. In THF and CH₂Cl₂, the (*R*)-phenylalanine derivative **7a** is obtained in 95% and 85% ee, respectively (Table 1, entries 2, 3). In the case where toluene or benzene is used, the enantioselectivities reach 97% or 98% ee, respectively (entries 4, 5). At last, when the reaction is performed under higher pressure (15 or 40 bar), the hydrogenated product is always obtained with full conversion, but with slightly lower ee, *i.e.*, 95% and 87%, respectively (Table 1, entries 6, 7).

The precatalyst **5a** was also investigated in the asymmetric hydrogenation of various substrates **6b–d** in benzene, and the experimental results are reported in Table 2. The hydrogenation of dimethyl itaconate **6b** under 1 bar of H₂ pressure in benzene affords the (*S*)-dimethyl 3-methylsuccinate **7b** in low conversion (10%, Table 2, entry 1). However, under 15 bar of hydrogen pressure, the conversion was total, and the product (*S*)-**7b** was obtained with ee up to 43% (entry 2). The hydrogenation of methyl 2-acetamidoacrylate **6c** under the same reaction conditions leads to the (*R*)-alanine derivative **7c** with lower enantioselectivity (ee 34%, entry 3). The calix[4]arenyl-AMP*P ligand **4a** was also used for the asymmetric hydrogenation of the industrial substrate **6d**, which is the precursor of levetiracetam, useful for the treatment of epilepsy and other neurological disorders.²⁸ When the

(27) (a) Ohkuma, T.; Kitamura, M.; Noyori, R. In *Catalytic Asymmetric Synthesis*, 2nd ed.; Ojima, I., Ed.; VCH Publishers Inc.: New York, 2000; pp 1–110. (b) Brown, J. M. In *Comprehensive Asymmetric Catalysis*; Jacobsen, E. N.; Pfaltz, A.; Yamamoto, H., Eds.; Springer: Berlin, 1999; Vol. 1, pp 121–182. (c) Nógrádi, M. *Stereoselective Synthesis*; VCH: Weinheim, 1987; p 53.

(28) Ates C.; Surtees, J.; Burteau, A. C.; Marmon, V.; Cavoy, E. WO 03/014080 A2, 2003.

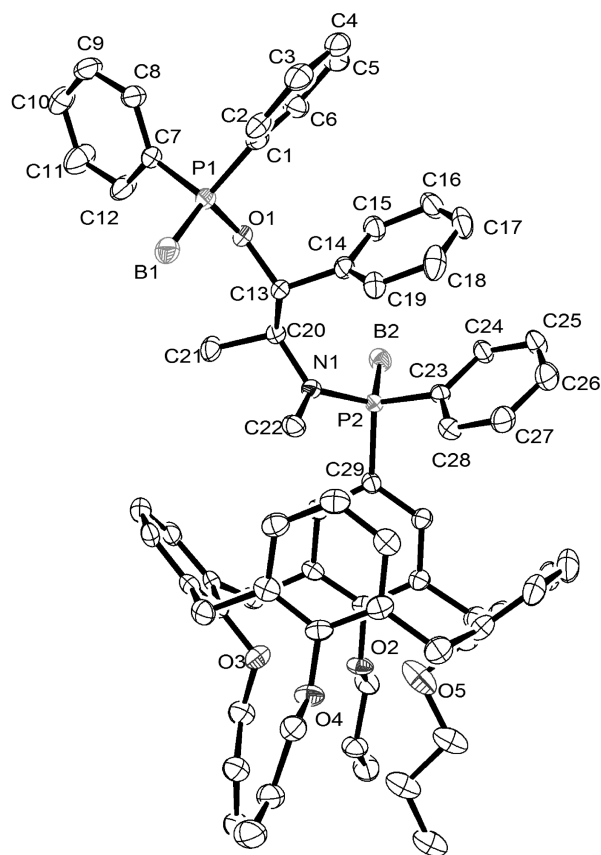


Figure 1. ORTEP view of the AMP*P-diborane complex **3a**. Thermal ellipsoids are set at the 50% probability level. Hydrogen atoms have been omitted for clarity. Selected bond lengths [Å], angles [deg], and dihedral angles [deg]: P1–B1 1.897(4), P2–B2 1.907(4), P2–N1 1.668(2), P1–O1 1.612(2); C20–N1–P2 121.5(2), C22–N1–P2 121.2(2); C22–N1–C20 116.5(2), B2–P2–N1–C22 170.9(2), B2–P2–C23–C24 7.7(3), O1–C13–C20–N1 178.9(2), B2–P2–C29–C30 97.8(3), B2–P2–C29–C34 85.3(3).

asymmetric hydrogenation of **6d** was performed in methanol or benzene under 15 bar of H_2 pressure, the reaction was total, and the product (*R*)-**7d** was obtained with 56% and 57% ee, respectively (entries 4, 5). Finally, the best asymmetric induction was obtained using THF as solvent, affording thus the hydrogenated product (*R*)-**7d** with 71% ee (entry 6).

In order to shine light on the role of the calix[4]arene substituent in this asymmetric induction, the hydrogenation of the substrates **6a–c** was performed in benzene and under 15 bar of H_2 pressure, using the Rh complexes **5a–c** prepared from the corresponding isoelectronic or sterically similar substituted AMP*P ligands **4a–c** (Table 3). In the presence of the complex **5a**, the methyl 2-acetamidocinnamate **6a** is hydrogenated to (*R*)-phenylalanine derivative **7a** with 95% ee (entry 1). Conversely, **5b** and **5c** give lower enantioselectivities of 66% and 47% ee, respectively (entries 2, 3). First, it should be noted that the asymmetric induction decreases in the presence of the propoxy group at the *para* position of the AMP*P substituent. Indeed, ligand **4c** leads to a lower ee than the 3,5-xylyl-substituted ligand **4b** (66% ee vs 47% ee, entries 2, 3). Surprisingly, this decreasing effect is likely overcome by the influence of the calix[4]arene substituent, bearing a propoxy at the *para* position, since the ligand AMP*P **4a** leads to 95% ee under the same conditions (entry 1). In the case of dimethyl itaconate **6b**, the asymmetric

Table 1. Asymmetric Catalyzed Hydrogenation of Methyl 2-Acetamidocinnamate (**6a**) in the Presence of [Rh(COD)(calix[4]arenyl-AMP*P **4a**)]BF₄ (**5a**)^{a,b}

entry	pH_2 (bar)	solvent	ee (%) ^{c,d}
1	1	MeOH	76
2	1	THF	95
3	1	CH ₂ Cl ₂	85
4	1	toluene	97
5	1	benzene	98
6	15	benzene	95
7	40	benzene	87

^a All reactions were carried out at room temperature with 3 mol % of Rh complex **5a** and 0.5 mmol of substrate. ^b In all cases, complete conversion was achieved. ^c Determined by HPLC with a Chiralcel OD-H column. ^d *R* absolute configuration.

hydrogenation in the presence of **5a** leads to (*S*)-dimethyl 3-methylsuccinate in 43% ee, whereas lower enantioselectivities are obtained with the complexes **5b** and **5c** (4% and 0% ee, respectively; entries 5, 6). Moreover, the benefic effect of the calix[4]arene AMP*P **4a** on the asymmetric catalysis is also observed for the industrial substrate **6d**, which affords the hydrogenated product **7d** with 57% ee, when the ligands **4b** and **4c** exhibit only 16 and 19% ee, respectively (entries 10–12). On the other hand, the asymmetric catalyzed hydrogenation of the methyl 2-acetamidoacrylate **6c** showed little significant effect of the *R*¹-substituents on the ligand, since the alanine derivative **7c** was obtained with enantiomeric excesses close to 37% for the AMP*P ligands **4a–c** (entries 7–9). Noteworthy, the comparison of the observed enantioselectivity for substrates **6a** and **6c** (*R*² = Ph and H, respectively) illustrates the importance of the phenyl group in the stereodetermining step. Indeed for substrate **6c**, no significant changes were observed in the enantioselectivity regardless of the nature of the AMP*P-containing ligand used (entries 1, 2, 3 vs 7, 8, 9).

In order to provide an explanation for the difference in asymmetric induction between the Rh complexes **5a**, **5b**, and **5c**, computer models were examined. Although the X-ray structure reveals the presence of the Rh fragment located outside the calix[4]arene cavity (Figure 2), the other possibility with the Rh moiety inside the cavity may exist based on the other complexes containing the calix[4]arene unit (Scheme 3a,b).^{20c}

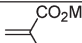
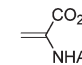
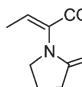
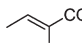
This is well exemplified in Figure 3 where two models of calix[4]arenyl-AMP*P/RhCl₂ were computed (*outer* and *inner*). The *outer* model exhibits the lowest calculated total energy (only by a slim value, 5.1 kJ mol^{−1}), consistent with the X-ray structure presented in Figure 2.

For the [Rh(COD)(calix[4]arenyl-AMP*P)]BF₄ complex **5a**, the elimination of the COD must also lead to a similar *outer/inner* equilibrium. For the *inner* conformation, the unsaturated rhodium complex **8** can be protected from solvent coordination by the shielding effect of the calix[4]arene cavity (Figure 3). It should be noted that the chirality of complex **8** in the *inner* conformation is obvious, as shown in the space-filling model (Figure 3, right). Finally, both conformations may exist and their relative population (*inner* vs *outer*) must depend on the coordinating solvent.

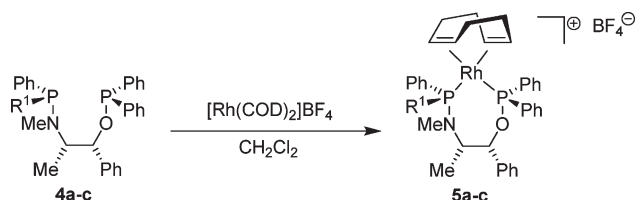
From a mechanistic point of view, this series of AMP*P ligands are interesting for the understanding of the interactions

Table 2. Asymmetric Catalyzed Hydrogenation of the Substrates **6b–d** in the Presence of Complex $[\text{Rh}(\text{COD})(\text{calix}[4]\text{-arenyl-AMP}^*\text{P})]\text{BF}_4$ (**5a**)^a

		$\begin{array}{c} \text{CO}_2\text{Me} \\ \\ \text{R}^2\text{C}=\text{C}-\text{Y}-\text{C}(\text{O})\text{R}^3 \\ \text{6a-d} \end{array} \xrightarrow[\text{pH}_2, \text{ solvent, RT}^\circ\text{C}]{[\text{Rh}(\text{COD})(\text{AMP}^*\text{P})]\text{BF}_4 \text{ 5a, 3\%}}$		$\begin{array}{c} \text{CO}_2\text{Me} \\ \\ \text{R}^2\text{CH}-\text{CH}_2-\text{Y}-\text{C}(\text{O})\text{R}^3 \\ \text{7a-d} \end{array}$			
		6,7	R ²	Y	R ³		
		a	Ph	NH	CH ₃		
		b	H	CH ₂	OMe		
		c	H	NH	CH ₃		
		d	Me	N(CH ₂) ₃			

Entry	Substrate	pH ₂ (bar)	Solvent	Conv. ^b (%)	Product	e.e. (%) ^c	Abs. conf.
1		1	benzene	10 ^d	7b	43	(S)
2	6b	15	benzene	100	"	43	(S)
3		15	benzene	100	7c	34	(R)
4		15	benzene	100	7d	57	(R)
5		15	MeOH	100	"	56	(R)
6	6d	15	THF	100	"	71	(R)

^a All reactions were carried out at room temperature with 3 mol % of Rh complex **5a** and 0.5 mmol of substrate. ^b Determined by ¹H NMR. ^c Determined by HPLC on a chiral column. ^d The reaction was carried out at 1 bar.

Scheme 2. Preparation of $[\text{Rh}(\text{COD})(\text{AMP}^*\text{P})]\text{BF}_4$ **5a**, **5b**, and **5c**.

occurring between the prochiral substrate and the Rh-(calix[4]arenyl-AMP*P) complexes **5**, **8**, and **9**, owing to the modification on the aminophosphine moiety. The modified AMP*P ligands **4b** and **4c**, bearing either the *m*-xylyl or *m*-dimethyl-*p*-propoxyphenyl substituent, respectively, afford lower asymmetric induction than **4a**. This observation rules in favor of the key role of the calix[4]arenyl moiety on the stereoselectivity. Multiple works focused on the origin of the enantioselectivity of the Rh-catalyzed hydrogenation, and for a long time, it was considered that the enantioselectivity does not stem from the relative stability of the substrate rhodium complexes, but from their rate constants of the oxidative addition of H₂ to the dihydro derivative (unsaturated route), such as **9** or **10**, respectively (Scheme 4).²⁹ However, other experimental and computational data supported a second reaction pathway *via* a fast equilibrium of the dihydride substrate complexes such as **10**, followed by the stereodetermining migration insertion step

leading to product **7** (Scheme 4).³⁰ Finally, the difference between the unsaturated and the dihydride pathway results mainly from the influence of the hydrogen pressure on the enantioselectivity. Thus, when the enantioselectivity was weakly influenced or decreased with an increase in hydrogen pressure, the former mechanism was invoked. Conversely, when the enantioselectivity increases with the hydrogen pressure, the stereodetermining step is the dihydro-rhodium-substrate complex **10** step (dihydro route).

Interestingly, when the hydrogenation of the substrate **6a** was performed at 1, 15, and 40 bar of H₂ pressure, using 3 mol % of $[\text{Rh}(\text{COD})(\text{AMP}^*\text{P})]\text{BF}_4$ **5a** complex, the (*R*)-*N*-acetylphenylalanine methyl ester **7a** was obtained with 98%, 95%, and 87% ee, respectively (Table 1, entries 5, 6, 7). Moreover for substrate **6b**, the Rh-catalyzed hydrogenation under 1 and 15 bar of hydrogen pressure leads to the product (*R*)-**7b** with the same enantioselectivity (Table 2, entries 1, 2). Consequently, these results are consistent with the mechanism using the unsaturated route presented in Scheme 4. In this case, the enantioselectivity is directed by the formation of the Rh-substrate complex **9**, where the presence of the calix[4]arenyl substituent plays an obvious role. It is reasonable to think that the complexation of substrate **6** with the unsaturated rhodium complex **8**, on the *re*- or the *si*-face, respectively, forces the corresponding complexes **9** to adopt the *outer* conformation for obvious steric reasons (Scheme 4).

(29) (a) Brown, J. M.; Chaloner, P. A. *J. Am. Chem. Soc.* **1980**, *102*, 3040–3048. (b) Chan, A. S. C.; Halpern, J. J. *J. Am. Chem. Soc.* **1980**, *102*, 838–840. (c) Chan, A. S. C.; Pluth, J. J.; Halpern, J. J. *J. Am. Chem. Soc.* **1980**, *102*, 5952–5954. (d) Chua, P. S.; Roberts, N. K.; Bosnich, B.; Okrasinski, S. J.; Halpern, J. J. *Chem. Commun.* **1981**, *102*, 1278–1280. (e) Landis, C. R.; Halpern, J. J. *J. Am. Chem. Soc.* **1987**, *109*, 1746–1754. (f) Nagel, U.; Rieger, B. *Organometallics* **1989**, *8*, 1534–1538. (g) Giovannetti, J. S.; Kelly, C. M.; Landis, C. R. *J. Am. Chem. Soc.* **1993**, *115*, 4040–4057. (h) Landis, C. R.; Hilfenhaus, P.; Feldgus, S. *J. Am. Chem. Soc.* **1999**, *121*, 8741–8754.

(30) (a) Landis, C. R.; Feldgus, S. *Angew. Chem., Int. Ed.* **2000**, *39*, 2863–2866. (b) Gridnev, I. D.; Higashi, N.; Asakura, K.; Imamoto, T. *J. Am. Chem. Soc.* **2000**, *123*, 7183–7194. (c) Giernoth, R.; Heinrich, H.; Adams, N. J.; Deeth, R. J.; Bargon, J.; Brown, J. M. *J. Am. Chem. Soc.* **2000**, *122*, 12381–12382. (d) Gridnev, I. D.; Imamoto, T. *Organometallics* **2001**, *20*, 545–549. (e) Heinrich, H.; Giernoth, R.; Bargon, J.; Brown, J. M. *J. Chem. Soc., Chem. Commun.* **2001**, 1296–1297. (f) Gridnev, I. D.; Higashi, N.; Imamoto, T. *Organometallics* **2001**, *20*, 4542–4553. (g) Gridnev, I. D.; Yasutake, M.; Higashi, N.; Imamoto, T. *J. Am. Chem. Soc.* **2001**, *123*, 5268–5376. (h) Crépey, K. V. L.; Imamoto, T. *Adv. Synth. Catal.* **2003**, *345*, 79–101. (i) Gridnev, I. D.; Imamoto, T. *Acc. Chem. Res.* **2004**, *37*, 633–644.

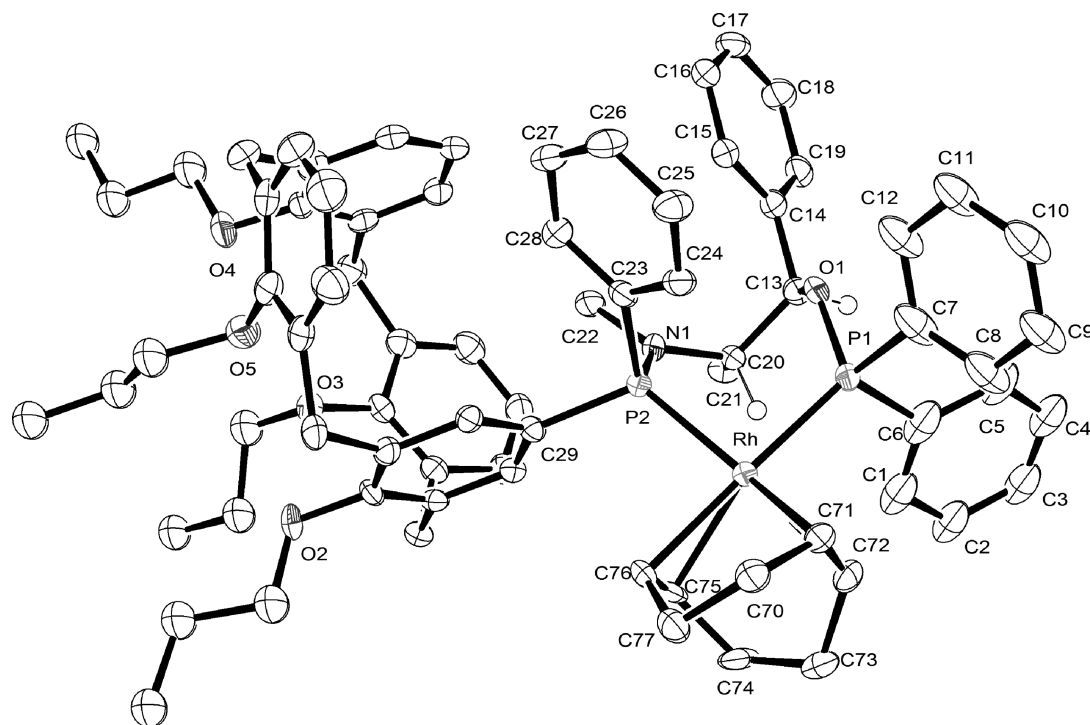


Figure 2. ORTEP view of the cationic $[(\text{COD})\text{Rh}(\text{AMP}^*\text{P})]\text{BF}_4$ complex **5a**. The thermal ellipsoids are at the 50% probability level. Hydrogen atoms, except for those located on C20 and C13 carbon atoms, BF_4 counterion, and solvent molecules, have been omitted for clarity. Selected bond lengths [Å], angles [deg], and dihedral angles [deg]: P1–O1 1.628(4), P2–N1 1.676(5), P1–Rh 2.2732 (10), P2–Rh 2.3146(13), Rh–HC20 2.913; P1–Rh–P2 91.18(5); O1–C13–N1–P2 $-12.71(38)$, P1–O1–C13–C14 $-179.23(32)$, P1–O1–C20–C21 $118.57(62)$, phenyl planes C7–C12 and C23–C28 $13.05(37)$.

Table 3. Asymmetric Rh-Catalyzed Hydrogenation Using the AMP^*P **4a–c**^{a,b}

Entry	Substrate	AMP*P	Rh-complexes	e.e. (%) ^c	Abs. conf.
1		4a	5a	95	(R)
2		4b	5b	66	(R)
3		4c	5c	47	(R)
4		4a	5a	43	(S)
5		4b	5b	4	(S)
6	6b	4c	5c	0	-
7		4a	5a	34	(R)
8		4b	5b	37	(R)
9		4c	5c	36	(R)
10		4a	5a	57	(R)
11		4b	5b	16	(R)
12		4c	5c	19	(R)

^a All reactions were carried out in benzene at room temperature with 3 mol % of catalyst **5a**, **5b**, or **5c** and 0.5 mmol of substrate, under 15 bar of H_2 . ^b In all cases, complete conversion was achieved. ^c Determined by HPLC (Chiralcel OD-H, OD).

Indeed, diastereomeric substrate–rhodium complexes **9** and **9'** are structurally completely different, and finally the presence of the bulky calix[4]arenyl substituent amplifies this difference with respect to the simple phenyl substituent on the phosphinite moiety (Scheme 4). A full analysis to address the relative amount or stability of substrate–rhodium complexes **9** and **9'** cannot be provided at this stage. Subsequently, the faster addition of hydrogen to complex **9** provides the corresponding

oxidatively added dihydro derivatives **10**, which ultimately leads to the major product **7** (Scheme 4). Noteworthy, the interaction model proposed for substrates **6a–d** in the coordination sphere of the rhodium complex **9** explains the enantioselectivity of the corresponding product **7**, *i.e.*, (*R*)-**7a**, (*S*)-**7b**, (*R*)-**7c**, and (*R*)-**7d** (Scheme 4). Finally, the rhodium complex **8**, reformed from the elimination of the hydrogenated product **7**, most likely adopts again the *inner* conformation prior to a subsequent complexation with another substrate, **6** (Scheme 4).

Conclusion

The first synthesis of a *P*-chirogenic aminophosphane–phosphinite (AMP^*P) ligand supported on the upper rim of a calix[4]arene moiety was achieved in two steps, using the ephedrine methodology. Two other AMP^*P models, bearing an isoelectronic or sterically similar substituent to the calix[4]arene fragment, were prepared using the same ephedrine methodology. These ligands were used in a Rh-catalyzed asymmetric hydrogenation of prochiral unsaturated substrates, reaching excellent activities and enantioselectivities up to 98% for the AMP^*P bearing the calix[4]arene substituent on the P-center. The enantioselectivity of the catalyzed hydrogenation, which was weakly influenced or slightly decreased with the hydrogen pressure, is consistent with the unsaturated route and a stereodetermining step involving the substrate–rhodium complexes. Computer models indicate the presence of two conformers for the active AMP^*P rhodium species, where the rhodium metal is either outside or inside the calix[4]arene cavity (*outer* or *inner*, respectively). It is obvious that the complexation of the substrate with the active rhodium species forces this one to completely

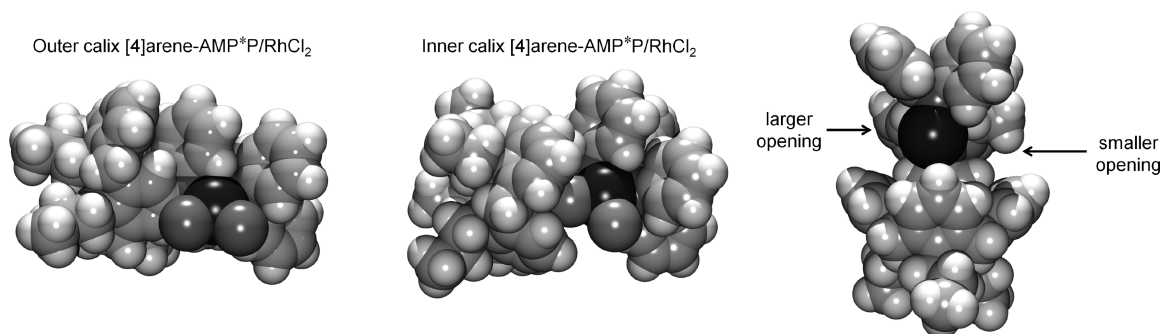
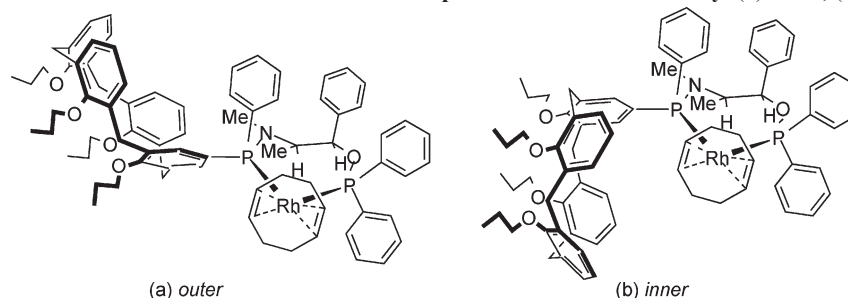
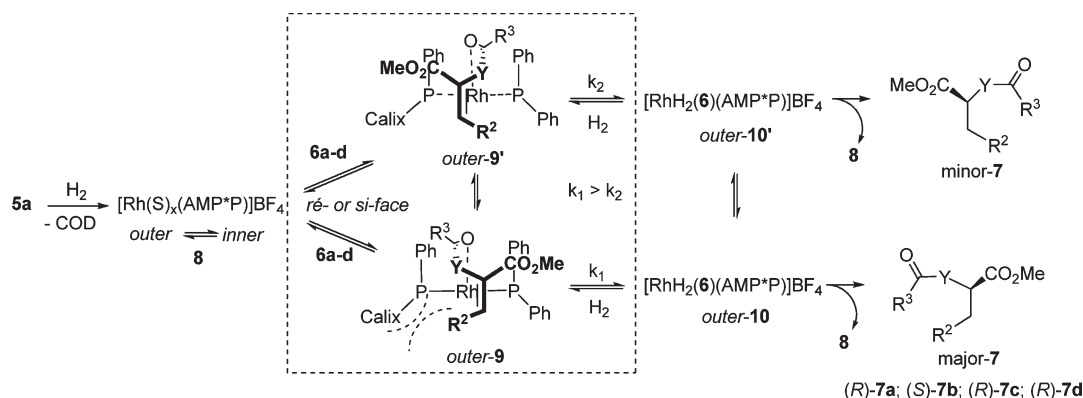


Figure 3. Left and center: Space-filling representation of the calix[4]arenyl-AMP*P/RhCl₂ computed models where the RhCl₂ unit is placed either outside (*outer*) or inside (*inner*) the cavity. Right: Space-filling model of the inner calix[4]arenyl-AMP*P/Rh computed model stressing the relative dimension of the opening on both sides of the intermediate structure and, therefore, chirality.

Scheme 3. Two Possible Conformations for Complex 5a with the Rh Moiety: (a) *outer*; (b) *inner*



Scheme 4



adopt the *outer* conformation. This process explains why the calixarene fragment plays a key role in the stereodetermining step.

Experimental Section

General Procedures. All reactions were carried out under an argon atmosphere in dried glassware with magnetic stirring. Solvents were dried prior to use. Tetrahydrofuran (THF), toluene, benzene, and diethyl ether (Et₂O) were distilled from sodium/benzophenone and stored under argon. Methanol (MeOH) was distilled from sodium. Dichloromethane (CH₂Cl₂) was distilled from CaH₂. Hexane and propan-2-ol for HPLC were of chromatographic grade and used without further purification. *s*-Butyllithium (1.4 M in cyclohexane), *tert*-butyllithium (1.6 M in pentane), 5-bromo-1,3-dimethylphenol, 1-bromo-*m*-xylene, BH₃·SMe₂, chlorodiphenylphosphane, α -acetamidocinnamic acid, α -acetamidoacrylic acid, trimethylsilyldiazomethane, dimethyl itaconate **6b**, and 1,4-diazabicyclo[2.2.2]octane (DABCO) were purchased from Aldrich, Acros, or Alfa Aesar and used as received. (+)- and (−)-Ephedrine were purchased from Aldrich

and dried by azeotropic shift of toluene on a rotary evaporator. [Rh(COD)₂]Cl₂ was purchased from Strem and used as received. The methyl α -acetaminocinnamate **6a** and methyl α -acetamidoacrylate **6c** were prepared from their corresponding acids, using trimethylsilyldiazomethane reagent.³¹ The substrate **6d** was prepared according to a literature procedure.³² The precatalyst complex [Rh(COD)₂]BF₄ was prepared following a modified procedure of Schrock and Osborn.³³ The 5-bromo-25,26,27,28-tetrapropoxycalix[4]arene³⁴ and 5-bromo-2-propoxy-1,3-dimethylphenyl³⁵ were prepared according to literature procedures.

(31) Presser, A.; Hüfner, A. *Monatsh. Chem.* **2004**, *135*, 1015–1022.

(32) (a) Ates, C.; Surtess, J.; Marmon, V.; Burteau, A. C.; Cavoy, E. PCT WO 03/014080 A2. (b) Surtess, J.; Marmon, V.; Differding, E.; Zimmermann, V. PCT WO 0164637 A1. (c) Schreiber, M. *J. Ann. Chim.* **1947**, 84–117.

(33) Schrock, R. R.; Osborn, J. A. *J. Am. Chem. Soc.* **1971**, *2397*–2407 and 3083–3091.

(34) Vézina, M.; Gagnon, J.; Villeneuve, K.; Drouin, M.; Harvey, P. D. *Organometallics* **2001**, *20*, 273–281.

(35) Larsen, M.; Krebs, F. C.; Harrit, N.; Jorgensen, M. *J. Chem. Soc., Perkin Trans. 2* **1999**, 1749–1757.

(2*R*,4*S*,5*R*)-(+)-3,4-Dimethyl-2,5-diphenyl-1,3,2-oxazaphospholidine-2-borane **1** was prepared from (–)-ephedrine, as previously described.³⁶ Reactions were monitored by thin-layer chromatography (TLC) using 0.25 mm E. Merck precoated silica gel plates. Visualization was accomplished with UV light and/or appropriate staining reagents. Flash chromatography was performed with the indicated solvents using silica gel 60 (particle size 0.035–0.070). NMR spectra (¹H, ¹³C, and ³¹P) were recorded on Bruker DRX 500 or Avance 300–600 MHz spectrometers. Chemical shifts are reported in ppm relative to 85% H₃PO₄ (³¹P) as an external standard. Data are reported as s = singlet, d = doublet, t = triplet, q = quartet, m = multiplet, br s = broad singlet, integration, coupling constant(s) in Hz. Melting points were measured on a Kofler bench melting point apparatus and are uncorrected. Optical rotation values were determined at 20 °C on a Perkin-Elmer 341 polarimeter. Mass spectral analyses were performed on a Bruker Daltonics microTOF-Q apparatus at Université de Bourgogne. Elemental analyses were measured at the Microanalysis Laboratory of the Université de Bourgogne.

(*S_P*)-(–)-{[(1*S*,2*R*)-2-(Diphenylphosphinitoborane)-1-methyl-2-phenylethyl](methyl)amino}{25,26,27,28-tetrapropoxycalix[4]arene}phosphaneborane, **3a**. A solution of *sec*-butyllithium (1.27 M in hexane, 2.6 mL, 3.3 mmol) was added under argon at –78 °C to a solution of 5-bromo-25,26,27,28-tetrapropoxycalix[4]arene (2 g, 3 mmol) in THF (6 mL). After 45 min, the mixture was added slowly to a solution of (+)-oxazaphospholidineborane **1** (941 mg, 3.3 mmol) in THF (6 mL). The reaction mixture was warmed to –40 °C and stirred for 2 h. When the starting complex **1** was totally consumed (TLC), the mixture was cooled to –78 °C and a solution of chlorodiphenylphosphane (1.1 mL, 6 mmol) was added. After 2 h at room temperature, borane dimethylsulfide (BH₃-DMS) (2.8 mL, 30 mmol) was added, and the mixture was stirred overnight. BH₃-DMS and THF were evaporated under reduced pressure, and the residue was hydrolyzed with water at 0 °C and then extracted with CH₂Cl₂. The organic layers were dried with anhydrous MgSO₄, and the solvent was removed. The residue was purified by column chromatography on silica gel using petroleum ether, then petroleum ether/ethyl acetate (9:1) as eluant to afford the AMP*P diborane **3a**, which was recrystallized with methanol (yield 62%). Suitable crystals for X-ray crystal structure determination were grown from dichloromethane/methanol at room temperature. White solid; mp = 157–160 °C. *R_f* = 0.43 (AcOEt/petroleum ether, 1:9). [α]_D²⁵ = +3.1 (c 1, CHCl₃). ¹H NMR (CDCl₃, 300 MHz): δ 7.70–7.50 (m, 2H, CH_{arom}), 7.50–7.40 (m, 3H, CH_{arom}), 7.30–6.80 (m, 17H, CH_{arom}), 6.70–6.50 (m, 4H, CH_{arom}), 6.40–6.20 (m, 5H, CH_{arom}), 5.10 (t, 1H, *J* = 9.3 Hz, CHO), 4.50 (AX system, 4H, *J* = 12.9 Hz, ArCH₂Ar), 4.40 (m, 1H, CHCH₃), 4.00 (m, 4H, CH₂O, OPr), 3.70 (m, 4H, CH₂O, OPr), 3.00 (AX system, 4H, *J* = 12.9 Hz, ArCH₂Ar), 2.00 (m, 4H, CH₂CH₃, OPr), 1.90 (m, 4H, CH₂CH₃, OPr), 1.40 (d, 3H, *J* = 7.1 Hz, CH₃N), 1.30 (d, 3H, *J* = 6.5 Hz, CH₃CH), 1.00 (td, 6H, *J* = 7.3, 0.8 Hz, CH₃, OPr), 0.90 (q, 6H, *J* = 7.5 Hz, CH₃, OPr). ¹³C NMR (CDCl₃, 75 MHz): δ 157.2 (d, *J* = 2.2 Hz, C_{arom}), 156.9 (d, *J* = 15.8 Hz, C_{arom}), 155.7 (s, C_{arom}), 138.0 (s, C_{arom}), 136.3 (d, *J* = 10.1 Hz, C_{arom}), 135.9 (d, *J* = 14.7 Hz, C_{arom}), 134.2 (d, *J* = 11.0 Hz, C_{arom}), 134.0 (d, *J* = 12.1 Hz, C_{arom}), 133.8 (d, *J* = 10.9 Hz, C_{arom}), 132.9 (s, C_{arom}), 132.6 (d, *J* = 12.2 Hz, CH_{arom}), 132.3 (s, C_{arom}), 131.9 (d, *J* = 10.8 Hz, CH_{arom}), 131.6 (s, CH_{arom}), 131.5 (s, CH_{arom}), 131.2 (d, *J* = 2.0 Hz, CH_{arom}), 131.1 (d, *J* = 11.1 Hz, CH_{arom}), 129.8 (br s, CH_{arom}), 128.9 (s, CH_{arom}), 128.6 (s, CH_{arom}), 128.5 (d, *J* = 11.0 Hz, CH_{arom}), 128.3 (s, CH_{arom}), 128.2 (s, CH_{arom}), 127 (s, CH_{arom}), 127.8 (d, *J* = 10.4 Hz, CH_{arom}), 127.7 (d, *J* = 4.4 Hz, CH_{arom}), 127.6 (d, *J* = 2.7 Hz, CH_{arom}), 122.6 (s, CH_{arom}), 122.4 (s, CH_{arom}), 122.2 (s, CH_{arom}), 82.9 (dd, *J* = 6.4, 2.7 Hz, CHO), 77.4 (s, CH₂O, OPr), 77.3 (s, CH₂O, OPr), 76.7 (s, CH₂O,

OPr), 76.6 (s, CH₂O, OPr), 57.4 (dd, *J* = 11.4, 8.2 Hz, CH-CH₃), 30.9 (s, ArCH₂Ar), 30.8 (s, ArCH₂Ar), 28.7 (d, *J* = 4.5 Hz, CH₃N), 23.4 (s, CH₂CH₃, OPr), 23.1 (s, CH₂CH₃, OPr), 23.0 (s, CH₂CH₃, OPr), 16.3 (s, CH₃CH), 10.6 (s, CH₃, OPr), 10.6 (s, CH₃, OPr), 10.0 (s, CH₃, OPr), 9.9 (s, CH₃, OPr). ³¹P NMR (CDCl₃, 121 MHz): δ 106.2 (P-O), 70.4 (P-N). ESI-MS: *m/z* (%) = 1098.6 (100) [M + Na]⁺, 1114.5 (18) [M + K]⁺. Anal. Calcd for C₆₈H₈₁B₂NO₅P₂ (1075.94): C, 75.91; H, 7.59; N, 1.30. Found: C, 75.69; H, 7.54; N, 1.30.

(*S_P*)-(–)-{[(1*S*,2*R*)-2-(Diphenylphosphinitoborane)-1-methyl-2-phenylethyl](methyl)amino}{[3,5-dimethyl-4-propoxy]phenyl}phosphaneborane, **3c**. This compound was prepared using the same procedure as for AMP*P **3a**, using 5-bromo-2-propoxy-1,3-dimethylphenyl (2 g, 8.22 mmol) to generate the corresponding organolithium reagent. Yield: 43%. White solid. Mp = 124–126 °C. *R_f* = 0.27 (toluene/petroleum ether, 1:1). [α]_D²⁵ = +58.6 (c 0.5, CHCl₃). ¹H NMR (CDCl₃, 300 MHz): δ 7.68–7.61 (m, 2H, CH_{arom}), 7.47–7.35 (m, 3H, CH_{arom}), 7.29–7.16 (m, 7H, CH_{arom}), 7.10–6.96 (m, 8H, CH_{arom}), 6.54 (td, 2H, *J* = 8.1, 1.2 Hz, CH_{arom}), 5.29 (t, 1H, *J* = 9.3 Hz, CHO), 4.48 (m, 1H, CHCH₃), 3.67 (t, 2H, *J* = 6.6 Hz, CH₂O, OPr), 2.20 (d, 3H, *J* = 7.8 Hz, CH₃N), 2.16 (s, 6H, CH₃Ar), 1.75 (m, 2H, CH₂CH₃, OPr), 1.25 (d, 3H, *J* = 6.6 Hz, CH₃CH), 0.99 (t, 3H, *J* = 7.2 Hz, CH₃, OPr). ¹³C NMR (CDCl₃, 75 MHz): δ 138.1 (s, C_{arom}), 133.2 (d, *J* = 11.2 Hz, CH_{arom}), 131.7 (d, *J* = 4.5 Hz, CH_{arom}), 131.6 (d, *J* = 5.9 Hz, CH_{arom}), 131.3 (s, CH_{arom}), 131.2 (s, C_{arom}), 131.1 (d, *J* = 11.2 Hz, CH_{arom}), 128.7 (s, CH_{arom}), 128.7 (d, *J* = 5.9 Hz, CH_{arom}), 128.5 (d, *J* = 4.4 Hz, CH_{arom}), 128.2 (s, CH_{arom}), 127.9 (d, *J* = 7.1 Hz, CH_{arom}), 127.8 (d, *J* = 7.2 Hz, CH_{arom}), 83.3 (dd, *J* = 11.9, 2.5 Hz, CHO), 73.8 (s, CH₂O, OPr), 57.3 (d, *J* = 15.4 Hz, CHCH₃), 29.3 (d, *J* = 4.1 Hz, CH₃N), 23.6 (s, CH₂CH₃, OPr), 16.5 (s, CH₃Ar), 16.2 (s, CH₃CH), 10.6 (s, CH₃, OPr). ³¹P NMR (CDCl₃, 121 MHz): δ 106.6 (P-O), 69.9 (P-N). ESI-MS: *m/z* (%) = 670.33 (100) [M + Na]⁺.

(*S_P*)-(–)-{[(1*S*,2*R*)-2-(Diphenylphosphinitoborane)-1-methyl-2-phenylethyl](methyl)amino}{[3,5-dimethyl]phenyl}phosphaneborane, **3b**. This compound was prepared by the same procedure as AMP*P **3a** using 1-bromo-3,5-dimethylphenyl (2 mL, 14.7 mmol) to generate the corresponding 3,5-dimethylphenyllithium. Yield: 34%. White solid. Mp = 193–195 °C. *R_f* = 0.28 (Et₂O/petroleum ether, 1:9). [α]_D²⁵ = +78.8 (c 1, CHCl₃). ¹H NMR (CDCl₃, 300 MHz): δ 7.68–7.61 (m, 2H, CH_{arom}), 7.46–7.35 (m, 3H, CH_{arom}), 7.30–7.16 (m, 6H, CH_{arom}), 7.08–6.96 (m, 10H, CH_{arom}), 6.54 (td, 2H, *J* = 8.1, 1.2 Hz, CH_{arom}), 5.30 (t, 1H, *J* = 9.3 Hz, CHO), 4.50 (m, 1H, CH₃CH), 2.22 (d, 3H, *J* = 6 Hz, CH₃N), 2.21 (s, 6H, CH₃Ar), 1.25 (d, 3H, *J* = 6.6 Hz, CH₃CH). ¹³C NMR (CDCl₃, 75 MHz): δ 138.1 (s, C_{arom}), 137.9 (d, *J* = 10.5 Hz, C_{arom}), 132.9 (d, *J* = 2.2 Hz, CH_{arom}), 132.9 (s, C_{arom}), 132.1 (d, *J* = 21.8 Hz, C_{arom}), 131.7 (s, CH_{arom}), 131.7 (d, *J* = 5.5 Hz, CH_{arom}), 131.6 (d, *J* = 7 Hz, CH_{arom}), 131.4 (d, *J* = 2.2 Hz, CH_{arom}), 131.1 (d, *J* = 11.3 Hz, CH_{arom}), 130.5 (d, *J* = 9.8 Hz, C_{arom}), 130.2 (d, *J* = 2.2 Hz, CH_{arom}), 130.1 (d, *J* = 10.4 Hz, CH_{arom}), 129.6 (d, *J* = 23.4 Hz, C_{arom}), 128.7 (s, CH_{arom}), 128.7 (d, *J* = 5.9 Hz, CH_{arom}), 128.5 (d, *J* = 3.3 Hz, CH_{arom}), 128.2 (s, CH_{arom}), 128.0 (d, *J* = 7.7 Hz, CH_{arom}), 127.9 (d, *J* = 7.7 Hz, CH_{arom}), 83.3 (dd, *J* = 8.9, 2.7 Hz, CHO), 57.3 (dd, *J* = 11.0, 8.7 Hz, CHCH₃), 29.4 (d, *J* = 4.3 Hz, CH₃N), 21.4 (s, CH₃Ar), 16.2 (s, CH₃CH). ³¹P NMR (CDCl₃, 121 MHz): δ 106.7 (P-O), 71.0 (P-N). ESI-MS: *m/z* (%) = 588.29 (100) [M – H]⁺. Anal. Calcd for C₃₆H₄₃B₂NOP₂ (589.30): C, 73.34; H, 7.30; N, 2.38. Found: C, 73.26; H, 7.46; N, 2.34.

(*S_P*)-(–)-{[(1*S*,2*R*)-2-(Diphenylphosphinito)-1-methyl-2-phenylethyl](methyl)amino}{25,26,27,28-tetrapropoxycalix[4]arene}phosphane, **4a**. To a solution of AMP*P diborane **3a** (0.28 g, 0.26 mmol) in 3 mL of toluene was added DABCO (0.12 g, 1.06 mmol), and the mixture was heated at 50 °C for 12 h. The crude product was rapidly filtered on a neutral alumina column using degassed dichloromethane as eluent. Yield: 98%. White solid. ¹H NMR (CDCl₃, 300 MHz): δ 7.50 (td, 2H, *J* = 7.8, 1.8 Hz, CH_{arom}), 7.40 (m, 3H, CH_{arom}), 7.30 (m, 2H, CH_{arom}), 7.20–7.10 (m, 8H,

(36) Bauduin, C.; Moulin, D.; Kaloun, E. B.; Darcel, C.; Jugé, S. *J. Org. Chem.* **2003**, *11*, 4293–4301.

CH_{arom}), 6.98 (td, 2H, $J = 7.9, 1.4$ Hz, CH_{arom}), 6.80 (dd, 1H, $J = 6.4, 2.1$ Hz, CH_{arom}), 6.70 (dd, 1H, $J = 6.5, 2.1$ Hz, CH_{arom}), 6.55 (m, 6H, CH_{arom}), 6.40 (dd, 2H, $J = 17.2, 7.1$ Hz, CH_{arom}), 6.35 (m, 4H, CH_{arom}), 4.70 (t, 1H, $J = 8.7$ Hz, CHO), 4.40 (AX system, 2H, $J = 13.1, 7.9$ Hz, $ArCH_2Ar$), 4.30 (A'X' system, 2H, $J = 12.9, 12.6$ Hz, $ArCH_2Ar$), 3.89 (t, 4H, $J = 7.8$ Hz, CH_2O , OPr), 3.78 (m, 1H, $CHCH_3$), 3.56 (td, 4H, $J = 5.2, 2.1$ Hz, CH_2O , OPr), 3.10 (AX system, 2H, $J = 17.7, 13.2$ Hz, $ArCH_2Ar$), 2.98 (A'X' system, 2H, $J = 17.9, 13.0$ Hz, $ArCH_2Ar$), 1.97 (m, 4H, CH_2CH_3 , OPr), 1.89 (m, 4H, CH_2CH_3 , OPr), 1.67 (d, 3H, $J = 2.8$ Hz, CH_3N), 1.22 (d, 3H, $J = 6.6$ Hz, CH_3CH), 0.99 (t, 6H, $J = 7.4$ Hz, CH_3 , OPr), 0.94 (q, 6H, $J = 7.5$ Hz, CH_3 , OPr). ^{13}C NMR ($CDCl_3$, 75 MHz): δ 155.6 (d, $J = 5.2$ Hz, C_{arom}), 155.1 (d, $J = 28.1$ Hz, C_{arom}), 141.3 (d, $J = 9.8$ Hz, C_{arom}), 141.1 (d, $J = 10.5$ Hz, C_{arom}), 140.2 (d, $J = 1.8$ Hz, C_{arom}), 137.7 (d, $J = 13.4$ Hz, C_{arom}), 136.7 (s, C_{arom}), 134.5 (br s, C_{arom}), 133.3 (d, $J = 9.3$ Hz, C_{arom}), 132.7 (d, $J = 6.2$ Hz, C_{arom}), 132.6 (d, $J = 5.4$ Hz, C_{arom}), 131.2 (d, $J = 20.1$ Hz, CH_{arom}), 131.2 (d, $J = 22.5$ Hz, CH_{arom}), 130.9 (s, CH_{arom}), 129.9 (d, $J = 22.7$ Hz, CH_{arom}), 129.3 (d, $J = 21.8$ Hz, CH_{arom}), 128.1 (d, $J = 17.6$ Hz, CH_{arom}), 127.6 (d, $J = 12.0$ Hz, CH_{arom}), 127.1 (br s, CH_{arom}), 126.8 (d, $J = 2.3$ Hz, CH_{arom}), 126.7 (d, $J = 3.1$ Hz, CH_{arom}), 126.4 (br s, CH_{arom}), 124.3 (s, CH_{arom}), 121.3 (s, CH_{arom}), 121.1 (d, $J = 9.3$ Hz, CH_{arom}), 85.4 (dd, $J = 18.1$ Hz, $J = 10.3$ Hz, CHO), 76.0 (s, CH_2O , OPr), 75.6 (s, CH_2O , OPr), 75.5 (s, CH_2O , OPr), 64.6 (dd, $J = 37.6, 7.3$ Hz, $CHCH_3$), 30.4 (d, $J = 9.8$ Hz, CH_3N), 29.8 (br s, CH_2 , $ArCH_2Ar$), 29.7 (s, CH_2 , $ArCH_2Ar$), 22.4 (s, CH_2CH_3 , OPr), 22.3 (s, CH_2CH_3 , OPr), 22.1 (s, CH_2CH_3 , OPr), 22.0 (s, CH_2CH_3 , OPr), 15.8 (d, $J = 4.64$ Hz, CH_3CH), 9.5 (s, CH_3 , OPr), 9.1 (s, CH_3 , OPr). ^{31}P NMR ($CDCl_3$, 121 MHz): δ 110.3 (P-O), 65.0 (P-N).

(S_P)-(–)-{[(1*S*,2*R*)-2-(diphenylphosphinito)-1-methyl-2-phenylethyl](methyl)amino}{[3,5-dimethyl-4-propoxy]phenyl}phosphane, **4c**. This compound was obtained from the decomplexation of **3c** (0.5 g, 0.77 mmol), using a similar procedure to that described for **4a**. Yield: 97%. White solid. 1H NMR ($CDCl_3$, 300 MHz): δ 7.45 (m, 2H, CH_{arom}), 7.24 (br s, 5H, CH_{arom}), 7.15–7.00 (m, 11H, CH_{arom}), 6.75 (d, 2H, $J = 7.5$ Hz, CH_{arom}), 6.61 (t, 2H, $J = 6.9$ Hz, CH_{arom}), 4.73 (t, 1H, $J = 9$ Hz, CHO), 3.85 (m, 1H, $CHCH_3$), 3.63 (t, 2H, $J = 6.6$ Hz, CH_2O , OPr), 2.10 (br s, 9H, CH_3Ar), 1.72 (m, 2H, CH_2CH_3 , OPr), 1.25 (d, 3H, $J = 6.6$ Hz, CH_3CH), 0.99 (t, 3H, $J = 7.5$ Hz, CH_3 , OPr). ^{13}C NMR ($CDCl_3$, 75 MHz): δ 156.6 (s, C_{arom}), 142.3 (d, $J = 12.1$ Hz, C_{arom}), 142.1 (d, $J = 13.2$ Hz, C_{arom}), 141.1 (d, $J = 1.8$ Hz, C_{arom}), 139.4 (d, $J = 10.5$ Hz, C_{arom}), 133.3 (d, $J = 21.8$ Hz, CH_{arom}), 133.3 (s, C_{arom}), 131.6 (d, $J = 18.1$ Hz, CH_{arom}), 131.1 (d, $J = 22.6$ Hz, CH_{arom}), 130.4 (s, C_{arom}), 130.3 (d, $J = 21.8$ Hz, CH_{arom}), 129.4 (s, CH_{arom}), 128.7 (s, CH_{arom}), 128.3 (br s, CH_{arom}), 127.9 (s, CH_{arom}), 127.7 (d, $J = 9.8$ Hz, CH_{arom}), 127.6 (d, $J = 9.0$ Hz, CH_{arom}), 86.6 (dd, $J = 18.1, 11.3$ Hz, CHO), 73.7 (s, CH_2O , OPr), 65.4 (dd, $J = 37, 7.5$ Hz, $CHCH_3$), 32.0 (d, $J = 9$ Hz, CH_3N), 23.7 (s, CH_2CH_3 , OPr), 17.0 (d, $J = 7.5$ Hz, CH_3CH), 16.4 (s, CH_3Ar), 10.7 (s, CH_3 , OPr). ^{31}P NMR ($CDCl_3$, 121 MHz): δ 110.4 (P-O), 63.5 (P-N).

(S_P)-(–)-{[(1*S*,2*R*)-2-(diphenylphosphinito)-1-methyl-2-phenylethyl](methyl)amino}{[3,5-dimethylphenyl]phenyl}phosphane **4c**. This compound was obtained from the decomplexation of **3c** (0.28 g, 0.47 mmol), using similar procedure as described for **4a**. Yield: 73%. White solid. 1H NMR ($CDCl_3$, 300 MHz): δ 7.45 (m, 2H, CH_{arom}), 7.25 (br s, 5H, CH_{arom}), 7.20–6.98 (m, 11H, CH_{arom}), 6.82 (br s, 1H, CH_{arom}), 6.71–6.62 (m, 4H, CH_{arom}), 4.75 (t, 1H, $J = 8.7$ Hz, CHO), 3.85 (m, 1H, $CHCH_3$), 2.13 (br s, 9H, CH_3Ar and CH_3N), 1.27 (d, 3H, $J = 6.6$ Hz, CH_3CH). ^{13}C NMR ($CDCl_3$, 75 MHz): δ 142.2 (d, $J = 12.07$ Hz, C_{arom}), 142.0 (d, $J = 12.8$ Hz, C_{arom}), 141.0 (d, $J = 1.5$ Hz, C_{arom}), 139.7 (d, $J = 11.3$ Hz, C_{arom}), 138.8 (d, $J = 15.8$ Hz, C_{arom}), 137.2 (d, $J = 6.8$ Hz, C_{arom}), 131.8 (d, $J = 18.8$ Hz, CH_{arom}), 131.3 (d, $J = 22.6$ Hz, CH_{arom}), 130.3 (d, $J = 15.8$ Hz, C_{arom}), 130.2 (s, CH_{arom}), 130.0 (d, $J = 12.1$ Hz, CH_{arom}), 129.3 (s, CH_{arom}), 128.7 (s, CH_{arom}), 128.3 (br s, CH_{arom}), 128.2 (s, CH_{arom}), 127.9 (d, $J = 1.5$ Hz, CH_{arom}), 127.7 (d, $J = 8.3$ Hz, CH_{arom}), 127.6 (d, $J = 1.5$ Hz, CH_{arom}), 86.5 (dd, $J = 18.1, 10.6$ Hz, CHO), 65.3 (dd, $J =$

37.7, 7.5 Hz, $CHCH_3$), 32.2 (d, $J = 9.8$ Hz, CH_3N), 21.3 (s, CH_3Ar), 17.1 (d, $J = 4.5$ Hz, CH_3CH). ^{31}P NMR ($CDCl_3$, 121 MHz): δ 110.5 (P-O), 63.6 (P-N).

(Cycloocta-1,5-diene)[(S_P)-(–)-{[(1*S*,2*R*)-2-(diphenylphosphinito)-1-methyl-2-phenylethyl](methyl)amino}{25,26,27,28-tetrapropoxycalix[4]arene}phosphane]rhodium Tetrafluoroborate, **5a**. A Schlenk tube was charged with AMP*P **4a** (0.29 g, 0.28 mmol) in freshly distilled dichloromethane (3 mL), and this solution was added at room temperature by cannula to a solution of $[Rh(COD)_2]BF_4$ (0.07 g, 0.17 mmol) in the dichloromethane (3 mL). The mixture was stirred at room temperature for 2 h, and the solvent was removed under reduced pressure to give an orange powder, which was crystallized from a CH_2Cl_2 /diethyl ether mixture to afford the corresponding complex as orange crystals. Yield: 92%. Mp = 228–230 °C. 1H NMR ($CDCl_3$, 300 MHz): δ 7.83 (m, 2H, CH_{arom}), 7.64 (m, 3H, CH_{arom}), 7.55 (m, 3H, CH_{arom}), 7.43–7.39 (m, 5H, CH_{arom}), 7.28–7.20 (m, 7H, CH_{arom}), 7.13 (m, 3H, CH_{arom}), 6.91 (d, 1H, $J = 7$ Hz, CH_{arom}), 6.84 (m, 1H, CH_{arom}), 6.62 (m, 5H, CH_{arom}), 6.50 (m, 1H, CH_{arom}), 5.86 (br s, 2H, CHO and $CHCH_3$), 5.01 (br s, 2H, COD), 4.8 (br s, 1H, COD), 4.72 (br s, 1H, COD), 4.41 (m, 4H, $ArCH_2Ar$), 4.01 (m, 4H, CH_2O), 3.62 (m, 4H, CH_2O), 3.43 (d, 1H, $J = 12.9$ Hz, $ArCH_2Ar$), 3.17 (d, 1H, $J = 12.9$ Hz, $ArCH_2Ar$), 3.03 (d, 1H, $J = 12.9$ Hz, $ArCH_2Ar$), 2.94 (d, 1H, $J = 12.9$ Hz, $ArCH_2Ar$), 2.88 (m, 1H, COD), 2.62 (m, 1H, COD), 2.31 (m, 6H, COD), 2.03 (m, 4H, CH_2CH_3 , OPr), 1.87 (m, 7H, CH_2CH_3 and CH_3N), 1.06 (m, 9H, CH_3CH and CH_3), 0.91 (m, 6H, CH_3 , OPr). ^{31}P NMR ($CDCl_3$, 121 MHz): δ 119.1 (d, $J = 179.3$ Hz, P-O), 91.4 (d, $J = 154.3$ Hz, P-N). ESI-MS: m/z (%) = 1258.48 (100) $[M - BF_4]^+$.

(Cycloocta-1,5-diene)[(S_P)-(–)-{[(1*S*,2*R*)-2-(diphenylphosphinito)-1-methyl-2-phenylethyl](methyl)amino}{[3,5-dimethyl-4-propoxy]phosphane}rhodium Tetrafluoroborate, **5c**. This complex was prepared by a similar procedure to that described for **5a**. Yield: 52%. Orange crystals. Mp = 128–130 °C. 1H NMR ($CDCl_3$, 300 MHz): δ 7.71 (m, 2H, CH_{arom}), 7.52 (m, 2H, CH_{arom}), 7.38 (m, 4H, CH_{arom}), 7.24 (m, 3H, CH_{arom}), 7.26–7.18 (m, 6H, CH_{arom}), 7.12–7.04 (m, 5H, CH_{arom}), 5.31 (m, 2H, CHO and $CHCH_3$), 4.57 (br s, 2H, COD), 4.46 (br s, 1H, COD), 4.34 (br s, 1H, COD), 3.66 (t, 2H, $J = 6.6$ Hz, CH_2O , OPr), 2.85 (m, 1H, COD), 2.52 (m, 1H, COD), 2.2 (m, 12H, CH_3Ar and COD), 1.89 (d, 3H, $J = 6.9$ Hz, CH_3N), 1.72 (m, 2H, CH_2CH_3 , OPr), 1.34 (d, 3H, $J = 6.9$ Hz, CH_3CH), 0.97 (t, 3H, $J = 4.5$ Hz, CH_3 , OPr). ^{31}P NMR ($CDCl_3$, 121 MHz): δ 120.0 (d, $J = 170.1$ Hz, P-O), 92.7 (d, $J = 164.0$ Hz, P-N). ESI-MS: m/z (%) = 830.28 (100) $[M - BF_4]^+$.

(Cycloocta-1,5-diene)[(S_P)-(–)-{[(1*S*,2*R*)-2-(diphenylphosphinito)-1-methyl-2-phenylethyl](methyl)amino}{[3,5-dimethylphenyl]phenyl}phosphane]rhodium Tetrafluoroborate, **5b**. This complex was prepared by a similar procedure to that described for **5a**. Yield: 66%. Orange crystals. Mp = 226–228 °C. 1H NMR ($CDCl_3$, 300 MHz): δ 7.89 (m, 2H, CH_{arom}), 7.53 (m, 4H, CH_{arom}), 7.40 (m, 3H, CH_{arom}), 7.28–7.20 (m, 6H, CH_{arom}), 7.08 (m, 4H, CH_{arom}), 6.96 (br s, 1H, CH_{arom}), 6.84 (m, 1H, CH_{arom}), 5.35 (m, 2H, CHO and $CHCH_3$), 4.58 (br s, 2H, COD), 4.47 (br s, 1H, COD), 4.34 (br s, 1H, COD), 2.85 (m, 1H, COD), 2.52 (m, 1H, COD), 2.23 (s, 6H, CH_3Ar), 2.14 (m, 6H, COD), 1.90 (d, 3H, $J = 6.6$ Hz, CH_3N), 1.35 (d, 3H, $J = 6.9$ Hz, CH_3CH). ^{31}P NMR ($CDCl_3$, 121 MHz): δ 120.0 (d, $J = 170.0$ Hz, P-O), 93.5 (d, $J = 162.8$ Hz, P-N). ESI-MS: m/z (%) = 772.23 (100) $[M - BF_4]^+$.

Typical Procedure for the Asymmetric Hydrogenation. A solution of $[Rh(COD)(AMP^*P)]BF_4$ **5a–c** (0.02 mmol, 3 mol %) and substrate **6** (0.59 mmol) in dry solvent (8 mL) was introduced in a stainless steel autoclave and stirred for 10 min. The autoclave was closed, purged with hydrogen, and then pressurized with hydrogen. After 16 h of stirring at room temperature, the pressure was released to atmospheric pressure and the solution was transferred to a round-bottom flask. The solvent was removed on a rotary evaporator to give a residue, which was purified by column chromatography on silica gel to

afford the hydrogenated product. The enantiomeric excess was determined by HPLC on a chiral column.

Methyl 2-Acetamido-3-phenylpropionate, 7a. The enantiomeric excess of **7a** was determined by HPLC on Chiralcel OD-H (25 cm): hexane/*i*-PrOH = 95:5, 1 mL/min, $t_R(R)$ = 21.4 min, $t_R(S)$ = 34.7 min. ^1H NMR (300 MHz, CDCl_3): δ 7.20 (m, 5H, CH_{arom}), 6.11 (br s, 1H, NHCOCH_3), 4.87 (m, 1H, CHCO_2CH_3), 3.64 (s, 3H, CO_2CH_3), 3.07 (m, 2H, CH_2Ph), 1.97 (s, 3H, COCH_3).

Dimethyl 3-Methylsuccinate, 7b. The enantiomeric excess of **7b** was determined by HPLC on Chiralcel OD (25 cm): hexane/*i*-PrOH = 95:5, 1 mL/min, $t_R(R)$ = 6.4 min, $t_R(S)$ = 11 min. ^1H NMR (300 MHz, CDCl_3): δ 3.62 (s, 3H, CO_2CH_3), 3.60 (s, 3H, CO_2CH_3), 2.85 (m, 1H, $\text{CH}_2\text{CO}_2\text{CH}_3$), 2.66 (dd, 1H, J = 16.5, 8.1 Hz, $\text{CH}_2\text{CO}_2\text{CH}_3$), 2.31 (dd, 1H, J = 16.5, 3 Hz, $\text{CH}_2\text{CO}_2\text{CH}_3$), 1.14 (d, 3H, J = 7.1 Hz, CHCH_3).

Methyl 2-Acetamidopropionate, 7c. The enantiomeric excess of **7c** was determined by HPLC on Chiralcel OD-H (25 cm): hexane/*i*-PrOH = 95:5, 1 mL/min, $t_R(R)$ = 19.9 min, $t_R(S)$ = 23.1 min. ^1H NMR (300 MHz, CDCl_3): δ 6.11 (br s, 1H, NHCOCH_3), 4.57 (m, 1H, CHCO_2CH_3), 3.72 (s, 3H, CO_2CH_3), 1.99 (s, 3H, NHCOCH_3), 1.36 (d, 3H, J = 6.8 Hz, CHCH_3).

Methyl 2-(2-Oxo-pyrrolidin-1-yl)butanoate, 7d. The enantiomeric excess of the **7d** was determined by HPLC on Chiralcel OD (25 cm): hexane/*i*-PrOH = 95:5, 1 mL/min, $t_R(S)$ = 18.5 min, $t_R(R)$ = 22.4 min. ^1H NMR (300 MHz, CDCl_3): δ 4.52 (dd, 1H, J = 10.5, 5.4 Hz, CHCO_2Me), 3.55 (s, 3H, CO_2CH_3), 3.35 (AB system, 1H, CH_2N), 3.20 (AB system, 1H, CH_2N), 2.28 (t, 2H, J = 8.1 Hz, CH_2CON), 1.88 (m, 3H, CH_2CH_3 and $\text{CH}_2\text{CH}_2\text{N}$), 1.52 (m, 1H, CH_2CH_3), 0.76 (t, 3H, J = 7.2 Hz, CH_2CH_3).

(37) (a) Otwinowski, Z.; Minor, W.; Carter, C. W., Jr. *Methods Enzymol.* **1997**, 276, 307–326. (b) Farrugia, L. *J. Appl. Crystallogr.* **1997**, 30, 565.

(38) Altomare, A.; Casciarano, G.; Giacovazzo, C.; Guagliardi, A. *J. Appl. Crystallogr.* **1993**, 26, 343–350.

(39) (a) Sheldrick, G. *Acta Crystallogr., Sect. A* **2008**, 64, 112–122. (b) *SHELX-97, Program for the Refinement of Crystal Structures*; Bruker AXS: Madison, WI, 1997.

Crystal Structure Determination. Diffraction data were collected on a Nonius Kappa CCD diffractometer equipped with a nitrogen jet stream low-temperature system (Oxford Cryosystems). The X-ray source was graphite-monochromated Mo K α radiation (λ = 0.71073 Å) from a sealed tube. The lattice parameters were obtained by least-squares fit to the optimized setting angles of the entire set of collected reflections. No significant temperature drift was observed during the data collections. Data were reduced by using DENZO³⁷ software without applying absorption corrections; the missing absorption corrections were partially compensated by the data scaling procedure in the data reduction. The structure was solved by direct methods using the SIR92³⁸ program. Refinements were carried out by full-matrix least-squares on F^2 using the SHELXL97³⁹ program on the complete set of reflections. Absolute configurations of all compounds were determined reliably from anomalous scattering, using the Flack method.⁴⁰

Computer Modeling. The computations were performed with PCModel version 7.0 from Serena Software.

Acknowledgment. This research was supported by the CNRS (Centre National de la Recherche Scientifique), the “Ministère de l’Education Nationale et de la Recherche”, the Natural Sciences and Engineering Research Council of Canada (NSERC), and Synthelabo S.A (Nancy). S.J. and P.D.H. are grateful to the Agence Nationale de la Recherche for funding (ANR BLAN *MetChirPhos*) and for an Excellence Research Chair held in Dijon.

Supporting Information Available: Crystallographic data in CIF format for compound **3a** and complex **5a**. This material is available free of charge via the Internet at <http://pubs.acs.org>.

(40) (a) Flack, H. *Acta Crystallogr., Sect. A* **1983**, 39, 876–881. (b) Flack, H. D. *Helv. Chim. Acta* **2003**, 86, 905–921. (c) Flack, H. D.; Bernardinelli, G. *J. Appl. Crystallogr.* **2000**, 33, 1143–1148.